Materials Research. 2017; 20(2): 326-338
DOI: http://dx.doi.org/10.1590/1980-5373-MR-2016-0318

The Development of Structure Model in Metallic Glasses

Xingxing Yue[a], Akihisa Inoue[b,c], Chain-Tsuan Liu[d], Cang Fan[a]*

[a]School of Material Science and Engineering, Engineering Research Center of Materials Behavior and Design Ministry of Education, Nanjing University of Science & Technology, 210094, Nanjing, Jiangsu Province, China
[b]International Institute of Green Materials, Josai International University, 283-8555, Togane, Chiba Province, Japan
[c]Department of Physics, King Abdulaziz University, 22254, Jeddah, Saudi Arabia
[d]Center for Advanced Structural Materials, Department of Mechanical and Biomedical Engineering – MBE, College of Science and Engineering, City University of Hong Kong, Hong Kong

Received: April 22, 2016; Revised: November 22, 2016; Accepted: December 13, 2016

Metallic glasses (amorphous alloys) have grown from a singular observation to an expansive class of alloys with a broad range of scientific interests. Their unique properties require a robust understanding on the structures at the atomic level while alloys in this class have a similar outlook on the microstructure. In this review, we went through the history of the majority studies on the structure models of metallic glasses, and summarized their historical contributions to the understanding of the structure metallic glasses and the relationship between their structures and properties.

Keywords: *Metallic glasses, Amorphous alloys, Structure model, Properties*

1. Introduction

Amorphous alloys were first synthesized in 1960 by Duwez and coworkers at the California Institute of Technology[1].

Metallic glasses, which show no long-range structural order, are usually referred to as amorphous alloys. After the first discovery of amorphous alloys, the scientists pay much attention to the new alloys because of their complex atomic structures and novel physical, mechanical and chemical properties[2-4], such as high electrical resistivity[5], soft-type superconductivity[6], good magnetic softness[7], high strength and large elastic strain[8,9]. These unusual properties make the amorphous alloys potentially useful for various applications.

Metallic glasses can be formed by quenching molten metals or alloys. Since the liquids tend to crystallize when the temperature (T) is below the melting temperature (T_m) or liquidus temperature (T_l), in order to retain the glassy structure, the cooling rate must be sufficiently fast to freeze the liquids before the crystals have the time to nucleate and grow. In this process, the liquids will undergo the glass transition at a temperature, called the glass transition temperature (T_g). The glass transition is a vital phenomenon. When a glassy solid is heated, the glass can be transferred to a supercooled liquid state at T_g. Here, the supercooled liquid refers to liquid at temperatures far below the melting points. In this process, it needs only very limited energy to get into the supercooled liquid compared with its crystallization process, but its physical and mechanical properties change dramatically[10,11]. Glass transition is so interesting that it almost always a hot topic in the papers[10,11] of studying the atomic structure of metallic glasses.

In the early 60s, the first metallic glass was obtained at very high cooling rates (10^5-10^6 *K/s*), resulting in a very limited thickness with only several tens micrometer. For the subsequent several decades, great effects have been devoted to decrease the critical cooling rate for glass formation. Even up to the late 1980s no significant achievements on reducing the critical cooling rate. However, in the late 80s and early 90s, metallic glasses were able to be produced at a much slower cooling rates[12-14]. Some metallic glasses have been produced at low cooling rates of around 1 *K/s* with sizes up to the range of 15 to 80 mm in diameter[15-22]. Such metallic glasses are so called as bulk metallic glasses (BMGs). The achievements of preparing BMGs in various alloy systems have dramatically accelerated the study on the glass-forming-ability and their fundamental properties. Following it, a three components rule which needs to be satisfied for forming BMGs was summarized in 1990s[23]: 1. the multicomponent system consisting of more than three elements, 2. significantly different atomic size ratios above about 12 % among the main three elements, 3. optimally large negative heats of mixing among the main three elements.

Meanwhile, over the past several decades, scientists have also made considerable efforts to explore atomic configurations in metallic glasses. It is well known that the atomic structure in crystalline solids shows a long-range translational periodicity. However, in metallic glasses, the long-rang order is absent

* e-mail: fan@njust.edu.cn

and no periodicity. For understanding the structure of metallic glasses, scientists have used extensive database to investigate their nature, proposing models at atomic level to characterize metallic glasses. With these studies, scientists found that metallic glasses can be characterized not only by randomness, but also short-range order (SRO), medium-range order (MRO) and efficient atomic packing around both solute and solvent atoms. SRO refers to the nearest-neighbor atomic environment. It contains the geometric short-range order and chemical short-range order[24-27]. At present, the study of SRO mostly focuses on the geometrical ordering. MRO refers to the second or third nearest -neighbor arrangement. The structure of MRO has a great influence on the formation and properties of metallic glasses.

Detailed structure information of metallic glasses can be generally inferred by the following two approaches: (1) Experiments such as X-ray diffraction (XRD)[28,29], extended X-ray absorption of fine structure (EXAFS)[30-32], small-angle X-ray scattering (SAXS)[33]; atom probe tomography[34], high-resolution transmission electron microscope (HREM)[35-37], synchrotron diffraction[38,39] and neutron scattering[40], (2) Computer simulation such as Monte Carlo simulation[41], Reverse Monte Carlo (RMC) simulation[42,43], Ab initio Molecular Dynamics (AIMD) simulation[44,45] and molecular dynamics (MD) simulation[46]. Based on the experiments and computer simulations, several structural models for the amorphous alloys have been proposed and successfully used to describe characteristics of metallic glasses from different perspectives. Models could not only give an intuitive image of structure, but also provide a foundation for developing high performance of new glassy materials. This paper mainly introduces the models, which were proposed in the last several decades, historically contributed to understanding the structure at atomic level and the relations between the structure and physical/mechanical properties of metallic glasses.

2. Structure models of metallic glasses

The atomic structure determines the intrinsic properties of metallic glasses. The disordered structure makes the metallic glasses possess unique physical/mechanical properties. We summarized the atomic structural models up to date and show them as follows.

2.1. Hard sphere random dense packing model

Compared with the structures of gas and crystalline solid, the structure model of liquid was mysterious for a long time. In1959, Bernal[47] first put forward a model to describe the structure of liquid called random dense packing model. This model mainly contains five Bernal polyhedrons[48] with edges of equal length, as shown in Figure 1, and their percentages are listed in Table 1. The tetrahedron accounts for about 73% of all Bernal polyhedrons and has the highest packing efficiency among the five polyhedrons, so the tetrahedron was considered as the most basic structure unit in the model. In 1960, he[49] further pointed out that a random dense packing of hard spheres resembles a monatomic liquid quite closely. In this model, the main assumptions are as follows: (1) the liquid is homogenous, coherent and irregular; (2) all the atoms are regarded as rigid balls and stacking without rules, and there is no extra hole whose size is an atom volume; (3) the atoms are incompressible. In 1964, Cohen and Turnbull[50] found that Bernal dense random model can describe the hypothetical metastable glassy state of simple liquids. Finney used Voronoi tessellation[51,52] to study the random dense packing model. He analyzed the 5500 Voronoi polyhedrons and found that the average face number of Voronoi polyhedra is 14.251 ± 0.015 and the average number of edges per face is 5.158 ± 0.003. This shows that there are a large number of pentagons in voronoi polyhedra. Five-rotating symmetry could not form the long-range order and hence the structures of Figures 1 (c), (d) and (e) are possible to form the amorphous alloy. In 1970, Cargill[53] compared the experimental pair distribution function (PDF) for noncrystalline Ni-P alloys with the distribution function for random dense packing of hard spheres and found that the feature was greatly similar. Besides, he pointed out that the random dense packing models may be useful in interpreting properties of amorphous alloys.

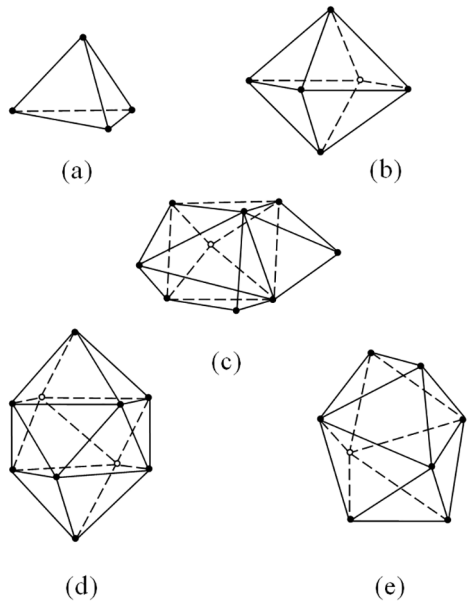

Figure 1. Five Bernal polyhedra: **(a)** Tetrahedron, **(b)** Octahedron; **(c)**Trigonal prism capped with three half octahedra; **(d)** Archimedean antiprism capped with two half octahedra; **(e)** Tetragonal dodecahedron.[48]

The PDF[54] is often used to describe and distinguish amorphous structure which is related to the probability of finding the center of a particle at a given distance from the center of another particle. For short distance, the PDF is related to the stack structure of particles. However, the curve

Table 1. The percentage of five Bernal polyhedrons.

Type	The number of percentage	Volume percentage
Tetrahedron	73%	48.4%
Octahedron	20.3%	26.9%
Trigonal prism capped with three half octahedra	3.2%	7.8%
Archimedean antiprism capped with two half octahedra	0.4%	2.1%
Tetragonal dodecahedron	3.1%	14.8%

of the PDF gradually converges to unity at a larger distance, showing the long-range disorder. The partial PDF is given by:

$$g_{\alpha\beta}(r) = \frac{1}{4\pi r^2 \rho N_\alpha N_\beta} \sum_{i=1}^{N_\alpha} \sum_{j=1, j+i}^{N_\beta} \delta(r - |\vec{r}_{ij}|) \qquad (1)$$

where ρ is the number density, N_α and N_β denote the number of α atoms and β atoms, respectively, $|\vec{r}_{ij}|$ is the interatomic distance between two atoms.

The total PDF is defined as:

$$g(r) = \frac{1}{4\pi r^2 \rho N} \sum_{i=1}^{N} \sum_{j=1, j+i}^{N} \delta(r - |\vec{r}_{ij}|) \qquad (2)$$

Figure 2 is the schematic illustration of PDF. The first peak (r: 3-5 Å) in the PDF is fairly sharp which derived from the atomic packing and configuration of the nearest-neighbor shell. The second, third, fourth, and fifth peaks are blunt but more pronounced than those found in liquids[55]. It is worthwhile to note that the split second peak (r: 5-10 Å) is usually found in metallic glasses. In addition, the radial distribution functions[56] (RDF) that describes how many α atoms within a distance of r and r + dr away from the β atom, can be calculated by means of PDF, namely:

$$\mathrm{RDF}(r) = 4\pi r^2 \rho_\beta g_{\alpha\beta}(r) \qquad (3)$$

where ρ_β is the number density of atom of type β.

Based on the random packing of hard spheres model, Polk's simulation results agreed well with the RDF obtained by experiments on metal-metalloid metallic glasses[57]. This model could explain why the metallic glasses cannot exhibit the long-range order structure in a certain extent and the RDF agrees well with the experimental results especially on metal-metalloid metallic glasses. The RDF[58,59] of the model was simulated and compared with the experimental results of Ni-P glassy alloys by Bennett et al. They found that the first peak suits well with the experimental result, but the second peak has certain differences. Sadoc et al.[60] adopted the two sizes of spheres heaps calculations, and assumed that the two small spheres did not touch. Their calculated values of some metallic glassy systems meet well with the experimental data, but the density is lower than the dense packing. In order to solve the contradiction between local structure of second peak and density, Connell[61], Baker et al.[62], Heimendhal[63] and Yamamoto[64] took the realistic interatomic potential into account based on the Bernal sphere-packing model. The modified model showed more agreement with the actual materials compared with the Bernal model. The

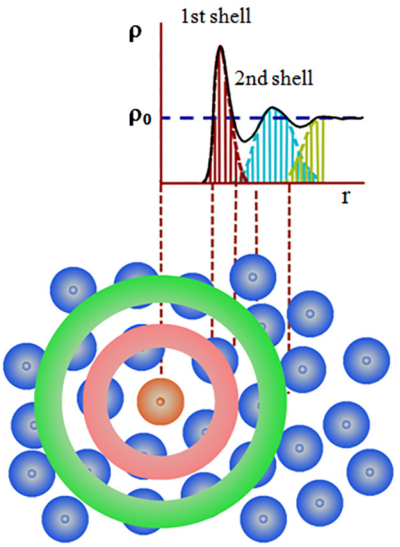

Figure 2. The illustration of pair distribution function.[56]

spheres are softened when considering the potential energy. According to the modern physics, we know that the atomic radius will change in the process of atomic interaction. So it is an important progress from hard spheres to soft spheres concept.

Simplifying the system and problems, mainly focusing on the geometry of the atomic arrangement, provides a very fundamental knowledge and is a very good start for studying atomic structures. The random dense packing model has reached certain achievements on the analysis of some metallic glassy systems, such as alloys with constituent species having comparable atomic sizes and insignificant chemical short-range order, contributing to understanding amorphous alloys at the atomic level, even people have been struggling to describe many binary metallic glasses, especially metal-metalloid alloys.

2.2. Micro-crystallite model

In 1947, Bragg[65] provided a dynamical model to describe the structure of crystal. He thought that the basic structure of metal consisted of small grains and grain boundaries. The model is called as micro-crystallite model. This model was initially used to describe the structure of liquid, since the structure of ambiguity is similar to the

liquid-like structure. Afterwards, Bagley et al.[66] used the micro-crystallite model to describe the configuration of amorphous alloys. A schematic illustration[67] of the model is given in Figure 3, which can explain some XRD data of certain metallic glasses. Inside of small grain, it exhibits the short-range order, which is similar to the crystal. These small grains are mixed randomly and their orientations are in disorder. It is therefore difficult to form the long-range ordered structure. The model can qualitatively explain some properties of amorphous alloys. However, the RDF is not agreement well with the experimental data. The details of the structures of microcrystalline area and boundary area are unknown, and furthermore the scientists also did not observe directly these areas in their experiments[68,69]. When the size of micro-crystallite is smaller, the volume of boundary will occupy too much and it is difficult to determine the atomic arrangements in associated areas. It is therefore regarded that this model does not fit the structures of metallic glasses.

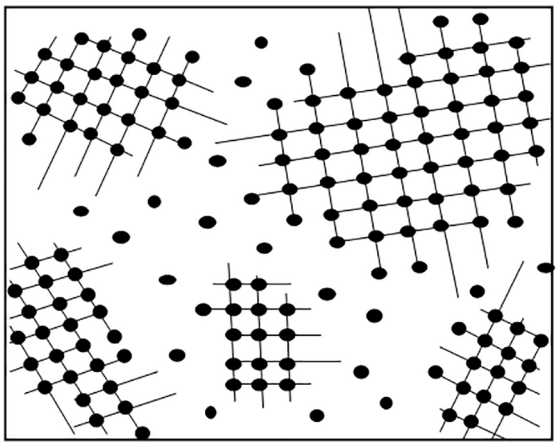

Figure 3. Micro-crystallite model.

2.3. Free volume model

Free volume model was put forward by Cohen and Turnbull[70-72] to explain the phenomenon of self-diffusion in Van der Waals liquids and liquid metals. Then Spaepen[73] developed this model by analysis of the mechanism for deformation and dynamics of metal in 1977, which can be used to describe the deformation and fracture of metallic glasses. He thought that there existed some free volumes in amorphous phase and the microscopic plasticity resulted from many single atom–jumps. When the liquid is cooled slowly, the atoms will rearrange and form the crystalline solid. In this process, the volume of material will shrink. On the other hand, when the liquid is quenched fast, the "gap" will be kept in amorphous solid. Its volume is larger than the corresponding crystalline solid and hence the increased part is called the free volume. In a word, the free volume V_f is defined as that part of the thermal expansion, or excess volume $\Delta\overline{V}$ which can be redistributed without energy change[72]. The term of the free volume is a very important concept and plays a significant role in amorphous alloys, and has been widely used to explain physical and mechanical properties of amorphous alloys. Figure 4 shows the process of atomic movement during deformation of metallic glasses and the creation of free volume, in which V^* is the effective hard-sphere size of the atom, ΔG^m is the activation energy of the motion, λ is the jump of length, τ is the shear stress, $\Delta G = \tau\Omega$ is the decreased free energy of the atom after jumping and Ω is the atomic volume.

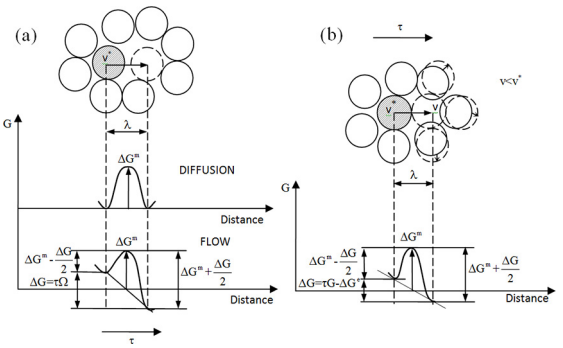

Figure 4. (a) Illustration of an atomic jump; **(b)** The creation of free volume.[73]

For an atom jump, it must have a nearest neighbor environment as shown in Figure 4 (a), and the nearby area also must have enough space to accommodate its atomic volume V^*. In this jumping process, the local free energy is minimal and some ΔG^m must be supplied. The number of jumps across the activation barrier is the same in both directions, when ΔG^m is obtained from thermal fluctuations. However, at an applied stress, the number of forward jumps across the activation barrier ($\Delta G^m - \frac{\Delta G}{2}$) is larger than that of backward jumps ($\Delta G^m + \frac{\Delta G}{2}$), and this results in a net forward flux of atoms and forms the basic mechanism for flow. Figure 4 (b) shows the creation of the free volume. Under the applied stress, the certain amount of free volume is created when an atom squeezes into a smaller space whose volume is V.

This model can analyze the flow behavior of metal glasses at high temperature. At low temperature, however, it cannot be well used to qualitatively analyze the deformation behavior of metallic glasses. The free volume model provides a simple and practical model to describe the plasticity of amorphous alloys. The applicability of the model has been well verified and it can qualitatively explain many mechanics properties of amorphous alloys[74-76]. In 1979, Argon[77] used "shear transformation" to explain the plastic deformation of metallic glasses and the theory meets well with the experimental observations. He thought that the "flow event" was not a single isolated event, but a rearrangement of a group of atoms. Falk[78,79] developed the theory of "shear transformation zone (STZ) " according to the molecular dynamics simulation in

conjunction with the complete mathematical model. An STZ only appears in response to external stimuli, being undefinable a priori in the static glass structure before deformation[80]. The shear transformation zone theory is an extension and expansion for free volume model at the molecular level. It can solve the defects of the free volume model, particularly in the description of low temperature state. But this process involves too many parameters. Based on the researches of Stillinger et al.[10,81], Malandro et al.[82] and Wales et al.[83,84], Johnson and Samwer[85] put forward the cooperative shear model (CSM). They well explained the plasticity behavior in low temperature.

2.4. Continuous random network model

Bernal's model has been widely accepted for metallic glasses, but it fails to describe the metal-metalloid-based alloys with pronounced chemical short-range order[86]. In light of this, Gaskell[87-89] put forward a model shown in Figure 5. He[87] thought that there was a basic structure unit that is similar to the corresponding component crystal microstructure in metallic glasses, this structure unit was regarded as tri-capped trigonal prism (TTP) that can form the net by coplanar points and coplanar faces. Figure 5(a) displays the regular trigonal prismatic coordination, in which N is the non-metallic element, M_I are metal atoms, M_{II} are further atoms capping the square faces at somewhat larger and even more variable M-N distances. For example, the TTP of Ni-P is P-centered and trigonal prism forms by six Ni atoms, another three Ni atoms capped the square faces of the prisms. Figure 5(b) shows a chain-like connection of trigonal prism by sharing edges. Dubois[90] proposed the packing rule of TTP based on the theory of chemical twinning. Gaskell[87] used this model to calculate the RDF of Pd-Si and found that it agreed well with the experimental data. However, there exist some limitations for describing the structure of metallic glasses[91-93]. For example, Waseda and Chen[91] found that the microstructure of Fe-B is different from that in Fe-P. Boudreaux and Frost[92] found two different structures (octahedron and trigonal prism) in Pd-Si, Fe-P and Fe-B with the help of computer simulation. So the TTP unit is not the only structure in metallic glasses. In addition, the model assumed that the neighbor bond length and angle are unchanged which make the system a smaller density than the corresponding component crystal. Thus it does not meet the principle of dense packing of metallic glasses, and the difference of densities obtained by theoretical calculation and experiment is obvious[94,95].

The model not only shows the homogeneity of metallic glasses macroscopicly, but also explains why the structure of the metallic glasses has long-range disorder. It reveals many properties such as isotropy, but cannot explain micro-inhomogeneity and phase splitting phenomenon of metallic glasses.

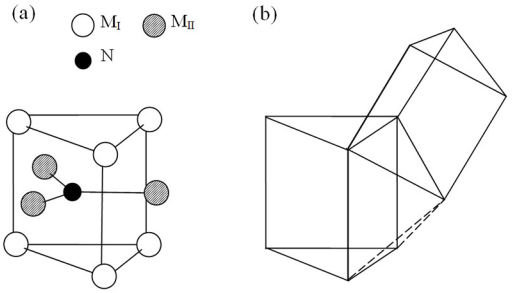

Figure 5. Gaskell's stereochemical model: **(a)** Regular trigonal prismatic coordination; **(b)** Edge-sharing of polyhedra.[87]

2.5. Dense packing of atomic cluster model

In the 1970s, Wang[96] suggested that amorphous alloys may have a crystal-like, short-range structure which retained by stacking various types of polyhedra and atomic disorders at random. These polyhedrons are called clusters those are considered as the basic unit in the structure of metallic glasses. They have more abundant atomic connection compared with the five basic Bernal polyhedrons[97,98]. In addition, the five-fold symmetry of the clusters can prevent the way of crystal growth to a certain extent. This is consistent with the principles of short-range order and long-range disorder in metallic glasses.

SRO is insufficient to describe the structure of metallic glasses and hence MRO is used to describe the connection and configuration of SRO. In order to describe the MRO of metallic glasses, Miracle[99,100] put forward the FCC/HCP dense packing cluster model in 2004. He put many hard spheres in a three-dimensional box and then made the spheres dense packing by shaking. He found that there exist many stable icosahedron clusters stacking in fcc. In this model, the center atom of cluster is regarded as solute atoms, and these atoms which occupied the gap of cluster are regarded as solvent atom. The model considers only three topologically distinct solutes and these solutes have specific and predictable sizes relative to the solvent atoms[101,102]. Figure 6 (a) shows an (110) plane of clusters in dense cluster-packing structure, which illustrates the feature of interpenetrating clusters and efficient atomic packing around each solute. And Ω is the solvent atom which is packed randomly, α is the primary cluster-forming solute species which usually form an fcc array extending to no more than a few cluster diameters, β is the secondary solute occupied the tetrahedral site and octahedral site. In this model, the solute-centered clusters with the solvent efficiently packed were considered as the basic building blocks and represented the SRO in metallic glasses. Furthermore, these clusters connected with each other by sharing the solvent atoms and formed the MRO. Figure 6 (b) shows the 3D Miracle dense cluster model for metallic glasses.

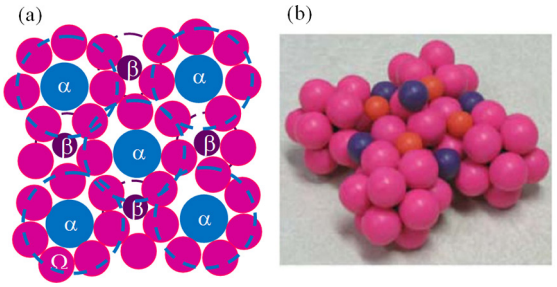

Figure 6. (a) 2D Miracle dense cluster model; **(b)** 3D cluster model.[99]

In Miracle's model, the order of the cluster-forming solutes cannot extend beyond a few cluster diameters, and hence the characteristic of disorder can be retained beyond the nanoscale. However, the model includes defects that provide rich structural description of metallic glasses. It could not only predict the number of solute atoms in the first coordination shell of a typical solvent atom, but also provide a remarkable ability to predict metallic-glass composition accurately for a wide range of simple and complex alloys. In general, this model is more successful in recent studies on glassy alloys.

According to the model of Miracle, Sheng et al.[103-105] used a combination of state-of-the-art experimental and computational techniques to analyze a range of binary systems and ternary systems that involve different atomic size ratios[106,107] and elucidate the different type of SRO as well as the nature of the MRO. They confirmed the dominance of solute-centered clusters and put forward a dense equivalent cluster packing model. They thought that the basic unit of metallic glasses is cluster made up of a variety of Voronoi polyhedra. Meanwhile they used Voronoi index method to measure the different clusters, then process statistical analysis. Voronoi index usually expresses as $<n_3,n_4,n_5,n_6, \ldots>$, n_i refers to the number i-edges faces of Voronoi polyhedra which can be considered as a characteristic signature of a particle's coordination structure. Since the face count is equal to the number of nearest neighbors of the particle, so $\sum_i n_i$ is called the coordination number (CN). For example, the icosahedral coordination structure corresponding to the Voronoi index <0,0,12,0, ... > describes a polyhedron with exactly 12 faces with 5 edges each. Figure 7 (a) shows the CN distribution in $Ni_{81}B_{19}$, $Ni_{80}P_{20}$, $Zr_{84}Pt_{16}$ and $Ni_{63}Nb_{37}$, respectively. The polyhedron structure in several representative metallic glasses is listed in Figure 7 (b). It can be seen that the average CN changes with the effective atomic size ratio radius (R*) between solutes and solvent atoms. The preference for a particular type of cluster is different with the variation of R* in various systems. When R* > 1.2, the main polyhedra belongs to the Frank-Kasper[108] type; when R* ≈ 0.902, the Frank-Kasper is transformed into the icosahedral type; when R* ≈ 0.835, the icosahedral type is transformed into the BSAP (bi-capped square Archimedean antiprism) type; when R* ≈ 0.732, the BSAP type is further transformed into the TTP type. The packing of solute-centered icosahedron cluster obtained by using the common-neighbor analysis[109] is displayed in Figure 8. It can be seen from this figure that the majorities of clusters are icosahedron (555) and icosahedron-like (544 and 433) clusters in $Ni_{81}P_{19}$, $Ni_{80}P_{20}$ and $Zr_{84}Pt_{16}$. Figure 8 (b) (c) (d) show the three typical cluster connections. In these figures,VS, ES and FS denote vertex-sharing, edge-sharing and face-sharing, respectively. In the same system, the type of cluster is similar, especially the type of topology and the coordination number.

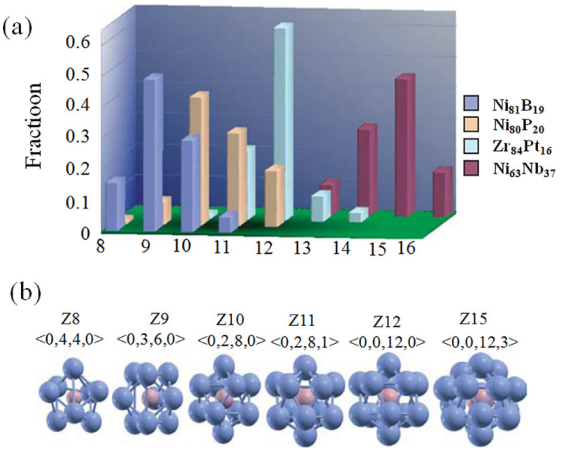

Figure 7. (a) The coordination number distribution of solute atoms in several metallic glasses; **(b)** The corresponding polyhedron structure.[103]

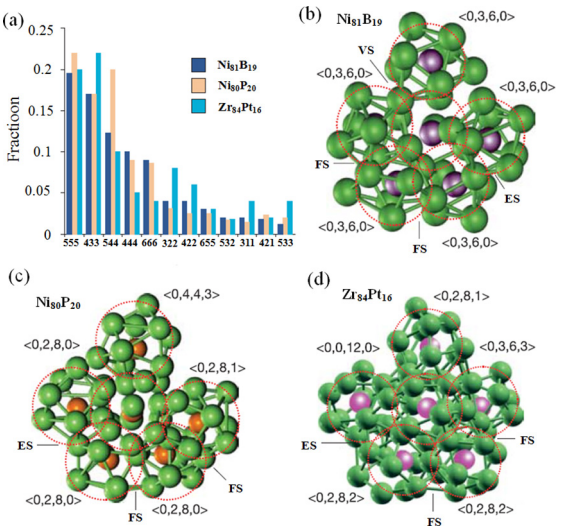

Figure 8. (a) The icosahedral type ordering of cluster in metallic glasses; **(b) (c)** and **(d)** The five-fold symmetry of cluster connections for $Ni_{81}B_{19}$, $Ni_{80}P_{20}$ and $Zr_{84}Pt_{16}$, respectively.[103]

The dense equivalent cluster packing model validates the important role of the effective atomic size ratio between the solute and solvent atoms and explicitly specifies the packing

topologies for various CNs. It greatly reduces the human subjective factor and the system error and enhances people's understanding of structure of metallic glasses.

Recently, based on the study of the Cu-Zr metallic glasses, Almyras et al.[110] found that the combinations of icosahedral-like clusters can be formed according to a simple rule. They demonstrated that the combinations of icosahedral-like clusters can follow a sequence of magic number by considering the system's stoichiometry. In experiments, the combinations of icosahedral-like clusters were referred to as "superclusters" and they regarded superclusters as basic building units[111]. Figure 9 shows a case of 20-atom supercluster composed of two 13-atom icosahedrons-like clusters, in which the brown spheres represent copper and the blue represent zirconium atoms. Their experimental results well agreed with the simulation and could reproduce the structural characteristics of the system. They suggested that the interconnections of clusters and consequently the formation of the superclusters were topological[112]. This method may be used to interpret the design of new metallic glasses and to understand their experimental data[113].

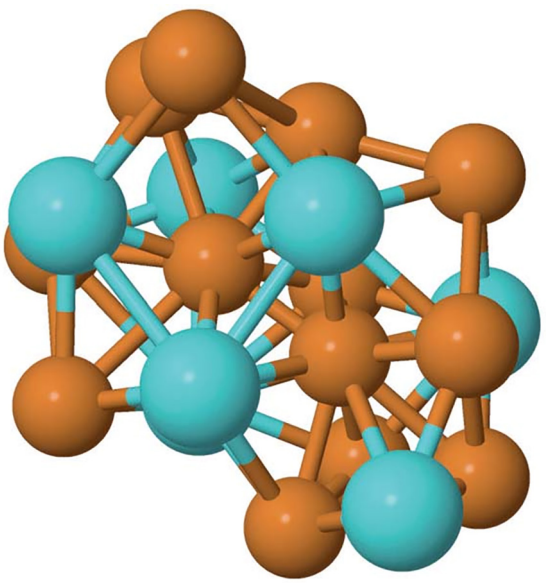

Figure 9. A case of 20-atom supercluster.[112]

2.6. Direct observation of the local structure in metallic glasses

Scientists did not directly observe the disordered structure of metallic glasses in experiments all the time. All the methods of studying the local structure of metallic glasses just provide the average and one-dimensional structural information. In 2010, Hirata et al.[114] investigated the configuration of metallic glass by nanobeam electron diffraction (NBED) combined with AIMD. They first directly observed the local atomic structure in metallic glasses. Figure 10 shows the experimental principle and structure image of metallic glasses.

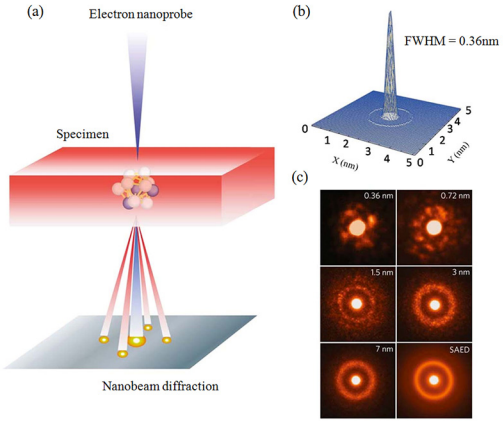

Figure 10. (a) The experimental principle; **(b)** The three-dimensional profile of a calculated electron nanoprobe with a FWHM beam size of ~0.36nm; **(c)** The image of local atomic order in metallic glasses.[114]

The direct observation provides an important method to explore the microstructure of metallic glasses by employing a state-of-the-art electron nanoprobe combined with AIMD simulation. Compared with the x-ray[115], extended x-ray absorption fine structure (EXAFS)[116] etc., this method can directly observe the distinct patterns from individual atomic cluster and its assemblies. This provides a new way to understand the properties and mechanisms of the metallic-glasses formation and gives a compelling evidence of short-range order in metallic glasses.

2.7. Flow unit model

In metallic glasses, there exist some different liquid-like regions and solid-like regions, as envisaged by Cohen and Grest[117,118]. In the system, the coordination of "liquid-like" atoms is unstable and changes within the Debye time, while the coordination of "solid-like" atoms has a long life-time[119]. Egami et al.[120] found that there exist about 24.3% liquid-like atoms in $Zr_{52.5}Cu_{17.9}Ni_{14.6}Al_{10}Ti_5$. Based on the researches of glassy structure and dynamic non-uniformity, Wang's team combines experiment with computer simulation. They have found that the liquid-like regions played a role of "detect", which can detect the atomic rearrangement and have characteristics of relatively high free energy, low density and viscoelasticity. The regions were defined as flow unit[121] in metallic glasses. Flow unit model is shown in Figure 11. In this model, they thought that the flow units as liquid-like quasi phases were embedded in solid-like glassy substrate[122,123].

The size of clusters in pink-color area is several nanometer level. Compared with other atoms in the metallic glass, they have low elastic modulus and strength, high liquidity and atomic energy, and atomic arrangement is looser. These areas are also known as "soft region" or "liquid-like regions", in which elastic energy cannot be stored, and they are embedded in a rigid metal glass substrate. When the metallic glasses

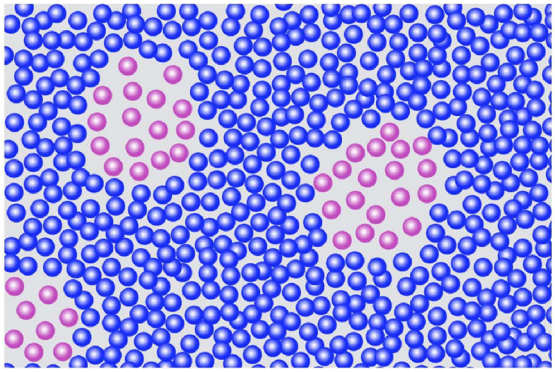

Figure 11. Flow unit model.[123]

are subject to stress or thermal activation, these areas will be rearranged and dissipate energy.

Different mechanical properties in metallic glasses result from the different characteristics of the flow units. For instance, the ductility in tension at 0.75 T_g achieved in the La-based MG is due to the activation of high density of flow units[124]. The fundamental flow units govern the mechanical behavior and ductility, and the activation energy and density of the flow units play a crucial role in the viscoelasticity and plasticity of metallic glasses. In addition, the features of the activated flow units are similar to those of the supercooled liquid, and the activation of flow units is the precursor of the glass transition.

This model can explain many phenomena in metallic glasses and also can help the understanding of some processes[125] such as the evolution of flow unit. Whether the flow units exist remains unclear, and needs a direct evidence from experiments.

2.8. Tight- bond cluster model

The high intense neutron scattering source for powder scattering, for example, the Neutron Powder Diffractometer (NPDF), provides a high resolution and a large Q-range (0.8 to 50 Å^{-1}), and together with low and stable background scattering, enables scientists to obtain excellent data for PDF studies of disordered and nanocrystalline materials. Taking this advantage, Fan et al. collected total-scattering for PDF on the as-cast and its crystallized counterpart of a Zr-Cu-Al ternary BMG at room temperature and cryogenic 15 *K*. They constructed an atomic model based on the peak spallation, atomic compression and tension appeared on the PDF data for the nearest atom pairs, in which strongly bonded clusters act as units or "hard spheres" instead of the individual atoms acting as hard spheres, and these clusters are randomly distributed, strongly connected, and result in free volume between the clusters[126]. They further developed the atomic model in 2009, and described it as the tight-bond cluster model. This model is illustrated in Figure 12 and contains essentially three major parts: (I) clusters of atoms with strong directional bonding (tight-bond clusters); (II) free-volume regions formed between the atomic clusters, in which atoms are loosely bonded; and (III) interconnecting zones with less directional bonding or transition bonding, which interconnect the clusters[127]. When $T< T_g$ (Figure 12a), the tightly bonded clusters randomly connected each other through the interconnecting zones and separated by the free volumes. When $T> T_g$, the tightly bonded clusters are completely separated by free volume (Figure 12b) as the interconnecting zones gaining energies become the free volumes (Figure 12c). At this stage, the cluster, i-zone and free volume concept were still based on qualitative definition.

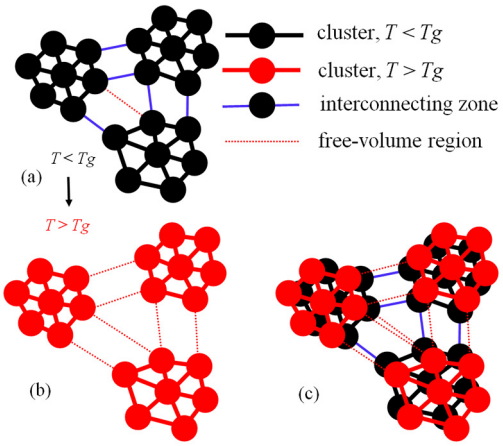

Figure 12. Tight-bond cluster model: A change in the connections between clusters below and above T_g (black: below T_g and red: above T_g).[128]

The properties of material always have an intimate relationship with their structure. In order to have a good understanding of the structure and the relationship between properties and structure in metallic glass, Fan et al.[127] built a sketch to illustrate the structural changes and try to explain the physical and mechanical properties of metallic glasses. As shown in Figure 13, A, B and C are represented as atomic clusters with different types or orientations. When the temperature rises close to the T_g, tight bonds in the interconnecting zones become loose as they gain energies, resulting in free volume. When the clusters are mostly separated by free volume, the solid amorphous structure is then transformed into the supercooled liquid state. So we can see that the high strength of metallic glasses results from the tight bond in the clusters. The interconnecting zone results in the formation of BMGs with high yield strength below T_g. The weakly bonded free-volume regions provide room for cooperative sliding and rotation of the clusters under applied loading, allowing clusters to move into layers of cooperative motion and resulting in shear-band formation and plastic deformation in BMGs at $T< T_g$. At $T> T_g$, all interconnecting zones are dissolved into the free-volume network, and tight-bond clusters could thus move easily

in the free-volume matrix, resulting in a homogeneous deformation under low applied stresses.

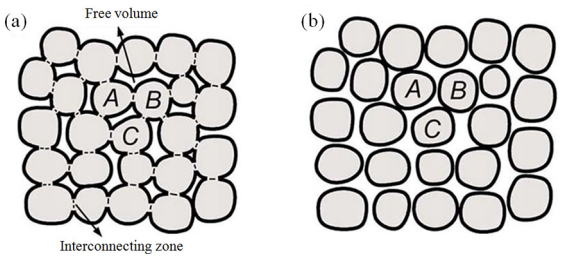

Figure 13. (a) When T< T_g, the clusters are connected to each other by interconnecting zone; **(b)** When T> T_g, the clusters are separated by free volume.[127]

In addition, Figure 14 shows a schematic illustration to further understand vividly the mutual relation among the three parts of the model proposed by Fan. The black-color parts represent the clusters, and the interconnecting zone between the clusters and the free volume region are shown in Figure 14 (b), and Figure 14 (c), respectively. The blue area in Figure 14 (b) represents the interconnecting zone between clusters, which may contain several layers of atoms. The atomic configuration in this interconnecting region is looser as compared with the cluster zones. The atoms marked with half blue and half red in Figure 14 (d) show the connecting state between atoms just near the clusters. The blue parts correspond to interconnection zones, while the red parts connect with the region belonging to free volume.

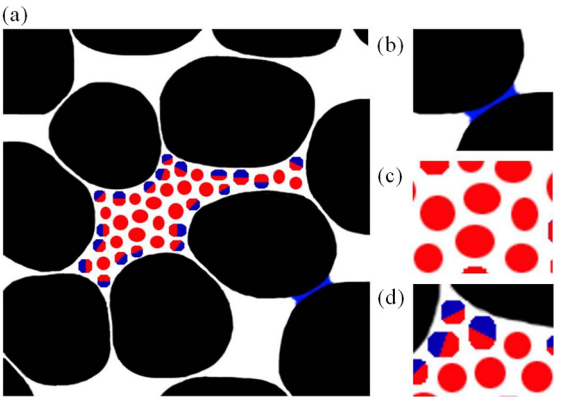

Figure 14. (a) Tight-bond cluster model; **(b)** The interconnecting zone between clusters; **(c)** Free volume zone; **(d)** The connecting condition between atoms in the boundary of clusters.

Based on a systematic study on PDF and RDF at different temperatures and phase states for ternary bulk metallic glasses[37,126,127-130], in 2015, they finally defined the free-volume, i-zone and cluster in metallic glasses for quantitatively understanding these concepts[129]. That is, (1) cluster: natural communities consist of strongly connected atoms, in which the bond distances of the nearest atoms are equal to or shorter than those within the crystal grains in the crystallized counterpart. (2) i-zone: areas consist of weak bonded atoms that have the bond lengths of the nearest atoms compared to those in the crystal boundaries in its crystallized counterpart. The bonding property in this area is similar to the crystal (grain) boundary in crystals. There are no crystals/grains, but clusters in metallic glasses. It is the reason why they use the concept of i-zone to describe the boundary-like area. The bond lengths in i-zone grow larger to form free volume network at glass transition temperature. (3) free volume: areas consists of the weakest bonded atoms that have the bond distances of the nearest atoms longer than those existed in its crystallized counterpart, i.e., the bond lengths of the nearest atoms are greater than that in the i-zone. Free-volumes do not exist in its crystallized counterpart and can be considered as supercooled liquid-like area. The authors also provided quantitative definition for the i-zone, and free-volume by distances between the nearest atoms in the as-cast $Zr_{55}Cu_{35}Al_{10}$ BMG. The initiating atom pair distances for i-zone and free volumes can be defined as that they are at least 2.8% greater, or at least 9.6% greater than that calculated from their characteristic atomic radius, respectively; and thus, the cluster is defined[128]. The authors claimed that the atoms which weakly connected i-zone should be one of the most dominated factors on mechanical properties in metallic glasses[40].

Based on the tight-bond model, these authors started to investigate the structural evolution and energy distribution of the Zr-, Cu- and Al-centered first shell clusters for $Zr_{55}Cu_{35}Al_{10}$ liquid and glass during the cooling process, and propose a new parameter to describe the structural evolution of the clusters[131]. In addition, they conducted series AIMD simulations to further analyze and improve their model[132]. Figure 15 shows the relative fractions of cluster, i-zone and free volume atom pairs compared to their summation as a function of temperature and Figure 16 shows the effect of different elements. They found that the relative fraction of the cluster atom pairs increases linearly and that of the free volume atom pairs decreases linearly with decreasing temperature. Although the radius of Al is not the smallest, it exerts a great influence on the structure of $Zr_{55}Cu_{35}Al_{10}$.

Although this model can well qualitatively explain many physical phenomena of amorphous alloys, it needs more research work on quantitatively determining the relationship between the mechanical properties and the atomic structures.

3. Conclusions

Scientists have made great efforts in studying the structure of amorphous alloys at the atomic level. Nowadays, we can say that the structures at the atomic-level of metallic glasses can be well understood with some mystery remaining. The lack of unit cells makes the amorphous structures much more complex at the atomic level and thus one of the important

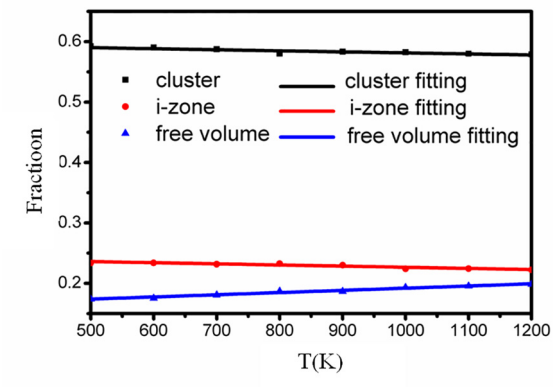

Figure 15. Changes of the relative fractions of cluster, i-zone and free volume atom pairs with temperature in AIMD simulations.[132]

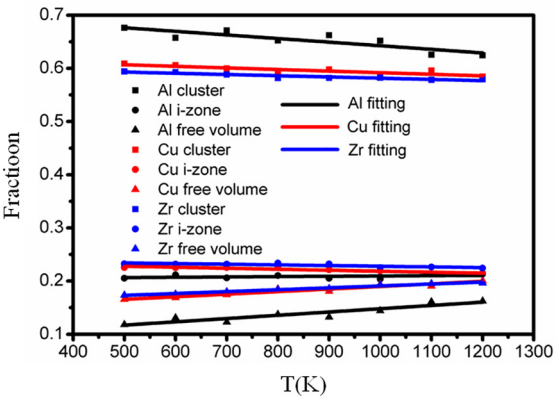

Figure 16. Changes of the relative fractions of Al, Cu and Zr cluster, i-zone and free volume atom pairs with temperature in AIMD simulations.[132]

interests to conduct further studies on their local atomic structures, which might be able to help scientists finally wipe the remaining mystery away. Furthermore, quantitatively characterizing and understanding the structure–property correlations at the atomic level on amorphous alloys are one of the most interesting topics, and also might be one of the hardest fields to finish, which is still attracting scientists greatly.

4. Acknowledgments

This work was supported by the NSFC (Grant No. 50971057 and 51371099). CTL is thankful for the financial support provided by the Research Grant Council (RGC), the Hong Kong Government through the General Research Fund (GRF) with the account number of City U 102013.

5. References

1. Klement Jun W, Willens RH, Duwez P. Non-crystalline Structure in Solidified Gold-Silicon Alloys. *Nature*. 1960;187(4740):869-870.

2. Chaudhari P, Turnbull D. Structure and properties of metallic glasses. *Science*. 1978;199(4324):11-21.

3. Qiao JC, Pelletier JM. Dynamic Mechanical Relaxation in Bulk Metallic Glasses: A Review. *Journal of Materials Science & Technology*. 2014;30(6):523-545.

4. Hufnagel TC, Schuh CA, Falk ML. Deformation of metallic glasses: Recent developments in theory, simulations, and experiments. *Acta Materialia*. 2016;109:375-393.

5. Inoue A, Zhang T, Kita K, Masumoto T. Mechanical Strengths, Thermal Stability and Electrical Resistivity of Aluminum-Rare Earth Metal Binary Amorphous Alloys. *Materials Transactions, JIM*. 1989;30(11):870-877.

6. Li Y, Bai HY, Wen P, Liu ZX, Zhao ZF. Superconductivity of bulk $Zr_{46.75}Ti_{8.25}Cu_{7.5}Ni_{10}Be_{27.5}$ metallic glass. *Journal of Physics*: *Condensed Matter*. 2003;15(27):4809-8415.

7. Inoue A, Takeuchi A. Recent progress in bulk glassy, nanoquasicrystalline and nanocrystalline alloys. *Materials Science and Engineering*: *A*. 2004;375-377:16-30.

8. Chen HS. Glassy metals. *Reports on Progress in Physics*. 1980;43(4):353-432.

9. Suryanarayana C, Inoue A. *Bulk metallic glasses*. Boca Raton: CRC Press; 2010. 565 p.

10. Debenedetti PG, Stillinger FH. Supercooled liquids and the glass transition. *Nature*. 2001;410(6825):259-267.

11. Lee KS, Ha TK, Ahn S, Chang YW. High temperature deformation behavior of the $Zr_{41.2}Ti_{13.8}Cu_{12.5}Ni_{10}Be_{22.5}$ bulk metallic glass. *Journal of Non-Crystalline Solids*. 2003;317(1-2):193-199.

12. Inoue A, Zhang T, Masumoto T. Al–La–Ni Amorphous Alloys with a Wide Supercooled Liquid Region. *Materials Transactions, JIM*. 1989;30(12):965-972.

13. Inoue A, Nakamura T, Nishiyama N, Masumoto T. Mg–Cu–Y Bulk Amorphous Alloys with High Tensile Strength Produced by a High-Pressure Die Casting Method. *Materials Transactions*, *JIM*. 1992;33(10):937-945.

14. Peker A, Johnson WL. A highly processable metallic glass: $Zr_{41.2}Ti_{13.8}Cu_{12.5}$ $Ni_{10.0}$ $Be_{22.5}$. *Applied Physics Letters*. 1993;63(17):2342-2344.

15. Inoue A, Nishiyama N, Matsuda T. Preparation of Bulk Glassy $Pd_{40}Ni_{10}Cu_{30}P_{20}$ Alloy of 40 mm in Diameter by Water Quenching. *Materials Transactions*, *JIM*. 1996;37(2):181-184.

16. Inoue A, Zhang T. Fabrication of bulk glassy $Zr_{55}Al_{10}Ni_5Cu_{30}$ alloy of 30 mm in diameter by a suction casting method. *Materials Transactions*, *JIM*. 1996;37(2):185-187.

17. Inoue A, Nishiyama N, Kimura H. Preparation and Thermal Stability of Bulk Amorphous $Pd_{40}Cu_{30}Ni_{10}P_{20}$ Alloy Cylinder of 72 mm in Diameter. *Materials Transactions*, *JIM*. 1997;38(2):179-183.

18. Johnson WL. Bulk Glass-Forming Metallic Alloys: Science and Technology. *MRS Bulletin*. 1999;24(10):42-56.

19. Zhang Q, Zhang W, Inoue A. Fabrication of New $Cu_{34}Pd_2Zr_{48}Ag_8Al_8$ Bulk Glassy Alloy with a Diameter of 30 mm. *Materials Transactions, JIM*. 2007;48(11):3031-3033.

20. Yuqiao Z, Nishiyama N, Inoue A. Development of Ni-Pd-PB Bulk Metallic Glasses with High Glass-Forming Ability. *Materials Transactions, JIM*. 2009;50(6):1243-1246.

21. Lou HB, Wang XD, Xu F, Ding SQ, Cao QP, Hono K, et al. 73 mm-diameter bulk metallic glass rod by copper mould casting. *Applied Physics Letters*. 2011;99(5):051910.

22. Nishiyama N, Takenaka K, Miura H, Saidoh N, Zeng Y, Inoue A. The world's biggest glassy alloy ever made. *Intermetallics*. 2012;30:19-24.

23. Inoue A. Recent Progress of Zr-Based Bulk Amorphous Alloys. *Science Reports of the Research Institutes, Tohoku University. Ser. A, Physics, Chemistry and Metallurgy*. 1996;42(1):1-11.

24. Cargill GS, Spaepen F. Description of chemical ordering in amorphous alloys. *Journal of Non-Crystalline Solids*. 1981;43(1):91-97.

25. Mattern N, Kühn U, Hermann H, Ehrenberg H, Neuefeind J, Eckert J. Short-range order of $Zr_{62-x}Ti_xAl_{10}Cu_{20}Ni_8$ bulk metallic glasses. *Acta Materialia*. 2002;50(2):305-314.

26. Huang L, Wang CZ, Hao SG, Kramer MJ, Ho KM. Short- and medium-range order in amorphous Zr_2Ni metallic alloy. *Physical Review B*. 2010;81(9):094118.

27. Ivison PK, Soletta I, Cowlam N, Cocco G, Enzo S, Battezzati L. Evidence of chemical short-range order in amorphous CuTi alloys produced by mechanical alloying. *Journal of Physics: Condensed Matter*. 1992;4(7):1635.

28. Nassif E, Lamparter P, Steeb S. X-ray Diffraction Study on the Structure of the Metallic Glasses Mg84Ni16 and Mg30Ca70. *Zeitschrift für Naturforschung A*. 1983;38(11):1206-1209.

29. Steeb S, Lamparter P. Diffraction studies of liquid and amorphous alloys. *Journal of Non-Crystalline Solids*. 1984;61-62(Pt 1):237-248.

30. Kaban I, Jóvári P, Escher B, Tran DT, Svensson G, Webb MA, et al. Atomic structure and formation of CuZrAl bulk metallic glasses and composites. *Acta Materialia*. 2015;100:369-376.

31. Sato S, Sanada T, Saida J, Imafuku M, Matsubara E, Inoue A. Effect of Al on Local Structures of Zr-Ni and Zr-Cu Metallic Glasses. *Materials Transactions*. 2005;46(12):2893-2897.

32. Enzo S, Schiffini L, Battezzati L, Cocco G. RDF and EXAFS structural study of mechanically alloyed $Ni_{50}Ti_{50}$. *Journal of the Less Common Metals*. 1988;140:129-137.

33. Cocco G, Enzo S, Antonione C, Riontino G, Venturello G. SAXS study of the structure of amorphous $Fe_{75}TM_5B_{20}$ (TM, Ti, V, Cr, Mn, Fe, Co, Ni). *Solid State Communications*. 1984;51(10):777-780.

34. Miller MK, Shen TD, Schwarz RB. Atom probe studies of metallic glasses. *Journal of Non-Crystalline Solids*. 2003;317(1-2):10-16.

35. He J, Kaban I, Mattern N, Song K, Sun B, Zhao J, et al. Local microstructure evolution at shear bands in metallic glasses with nanoscale phase separation. *Scientific Reports*. 2016;6:25832.

36. Ichitsubo T, Matsubara E, Yamamoto T, Chen HS, Nishiyama N, Saida J, et al. Microstructure of fragile metallic glasses inferred from ultrasound-accelerated crystallization in Pd-based metallic glasses. *Physical Review Letters*. 2005;95(24):245501.

37. Fan C, Liu CT, Chen G, Chen G, Liaw PK, Yan HG. Effect of molten quenching temperature on glass-forming ability of nanoquasi-crystal-forming Zr-based metallic glasses. *Scripta Materialia*. 2013;68(7):534-537.

38. Mattern N, Bednarčik J, Pauly S, Wang G, Das J, Eckert J. Structural evolution of Cu–Zr metallic glasses under tension. *Acta Materialia*. 2009;57(14):4133-4139.

39. Michalik S, Michalikova J, Pavlovic M, Sovak P, Liermann HP, Miglierini M. Structural modifications of swift-ion-bombarded metallic glasses studied by high-energy X-ray synchrotron radiation. *Acta Materialia*. 2014;80:309-316.

40. Fan C, Liu CT, Chen G, Liaw PK. Quantitatively defining free-volume, interconnecting- zone and cluster in metallic glasses. *Intermetallics*. 2015;57:98-100.

41. Luo SY, Li JH, Cui YY, Liu BX. Glass-formation and atomic structures of $Cu_x(Zr_{0.22}Hf_{0.78})_{1-x}$ and $(Cu_{0.61}Hf_{0.39})_{1-x}$ Zr_x alloys investigated by Monte Carlo simulation. *Materials Letters*. 2013;100:130-132.

42. McGreevy RL, Pusztai L. Reverse Monte Carlo Simulation: A New Technique for the Determination of Disordered Structures. *Molecular Simulation*. 1988;1(6):359-367.

43. Keen DA, McGreevy RL. Structural modelling of glasses using reverse Monte Carlo simulation. *Nature*. 1990;344(6265):423-425.

44. Kresse G, Hafner J. *Ab initio* molecular dynamics for liquid metals. *Physical Review B*. 1993;47(1):558.

45. Kresse G. Ab initio molecular dynamics for liquid metals. *Journal of Non-Crystalline Solids*. 1995;192-193:222-229.

46. Trady S, Mazroui M, Hasnaoui A, Sassouni K. Molecular dynamics study of atomic-level structure in monatomic metallic glass. *Journal of Non-Crystalline Solids*. 2016;443:136-142.

47. Bernal JD. A Geometrical Approach to the Structure of Liquids. *Nature*. 1959;183(4655):141-147.

48. Bernal JD. Geometry of the Structure of Monatomic Liquids. *Nature*. 1960;185(4706):68-70.

49. Bernal JD, Mason J. Packing of Spheres: Co-ordination of Randomly Packed Spheres. *Nature*. 1960;188(4754):910-911.

50. Cohen MH, Turnbull D. Metastability of Amorphous Structures. *Nature*. 1964;203(4948):964.

51. Finney JL. Random packings and the structure of simple liquids. I. The geometry of random close packing. *Proceedings of the Royal Society of London A: Mathematical, Physical and Engineering Sciences*. 1970;319(1539):479-493.

52. Finney JL. Modelling the structures of amorphous metals and alloys. *Nature*. 1977;266(5600):309-314.

53. Cargill GS. Dense Random Packing of Hard Spheres as a Structural Model for Noncrystalline Metallic Solids. *Journal of Applied Physics*. 1970;41(5):2248-2250.

54. Faber TE, Ziman JM. A theory of the electrical properties of liquid metals. *Philosophical Magazine*. 1965;11(109):153-173.

55. Bennett CH. Serially Deposited Amorphous Aggregates of Hard Spheres. *Journal of Applied Physics*. 1972;43(6):2727-2734.

56. Wang WH. The nature and properties of amorphous matter. *Progress in Physics*. 2013;33(5):177-351.

57. Polk DE. The structure of glassy metallic alloys. *Acta Metallurgica*. 1972;20(4):485-491.

58. Adams DJ, Matheson AJ. Computation of Dense Random Packings of Hard Spheres. *The Journal of Chemical Physics*. 1972;56(5):1989-1994.

59. Matheson AJ. Computation of a random packing of hard spheres. *Journal of Physics C: Solid State Physics*. 1974;7(15):2569-2576.

60. Sadoc JF, Dixmier J, Guinier A. Theoretical calculation of dense random packings of equal and non-equal sized hard spheres applications to amorphous metallic alloys. *Journal of Non-Crystalline Solids*. 1973;12(1):46-60.

61. Connell GAN. Dense random packings of hard and compressible spheres. *Solid State Communications*. 1975;16(1):109-112.

62. Barker JA, Hoare MR, Finney JL. Relaxation of the Bernal model. *Nature*. 1975;257(5522):120-122.

63. Heimendhal LV. Metallic glasses as relaxed Bernal structures. *Journal of Physics F: Metal Physics*. 1975;5(9):L141.

64. Yamamoto R, Matsuoka H, Doyama M. Structural relaxation of the dense random packing model for amorphous iron. *Physica Status Solidi (a)*. 1978;45(1):305-314.

65. Bragg L, Nye JF. A dynamical model of a crystal structure. *Proceedings of the Royal Society of London A*: *Mathematical*, *Physical and Engineering Sciences*. 1947;190(1023):474-481.

66. Bagley BG, Turnbull D. Structure Study of an Amorphous Electrodeposited Nickel-Phosphorus Alloy. *Journal of Applied Physics*. 1968;39(12):5681-5685.

67. Waseda Y. *The Structure of Non-Crystalline Materials: Liquids and Amorphous Solids*. New York: McGraw-Hill; 1980. 326 p.

68. Wagner CNJ. Structure of Amorphous Alloy Films. *Journal of Vacuum Science and Technology*. 1969;6(4):650-657.

69. Cargill GS III. Structure Investigation of Noncrystalline Nickel-Phosphorus Alloys. *Journal of Applied Physics*. 1970;41(1):12-29.

70. Cohen MH, Turnbull D. Molecular transport in liquids and glasses. *The Journal of Chemical Physics*. 1959;31(5):1164.

71. Turnbull D, Cohen MH. On Free-Volume Model of Liquid-Glass Transition. *The Journal of Chemical Physics*. 1970;52(6):3038.

72. Turnbull D, Cohen MH. Free-Volume Model of the Amorphous Phase: Glass Transition. *The Journal of Chemical Physics*. 1961;34(1):120.

73. Spaepen F. A microscopic mechanism for steady state inhomogeneous flow in metallic glasses. *Acta Metallurgica*. 1977;25(4):407-415.

74. de Hey P, Sietsma J, van Den Beukel A. Structural disordering in amorphous $Pd_{40}Ni_{40}P_{20}$ induced by high temperature deformation. *Acta Materialia*. 1998;46(16):5873-5882.

75. Flores KM, Sherer E, Bharathula A, Chen H, Jean YC. Sub-nanometer open volume regions in a bulk metallic glass investigated by positron annihilation. *Acta Materialia*. 2007;55(10):3403-3411.

76. Hajlaoui K, Benameur T, Vaughan G, Yavari AR. Thermal expansion and indentation-induced free volume in Zr-based metallic glasses measured by real-time diffraction using synchrotron radiation. *Scripta Materialia*. 2004;51(9):843-848.

77. Argon AS. Plastic deformation in metallic glasses. *Acta Metallurgica*. 1979;27(1):47-58.

78. Falk ML, Langer JS. Dynamics of viscoplastic deformation in amorphous solids. *Physical Review E*. 1998;57(6):7192-7205.

79. Langer JS. Shear-transformation-zone theory of deformation in metallic glasses. *Scripta Materialia*. 2006;54(3):375-379.

80. Greer AL, Cheng YQ, Ma E. Shear bands in metallic glasses. *Materials Science and Engineering: R: Reports*. 2013;74(4):71-132.

81. Stillinger FH. Supercooled liquids, glass transitions, and the Kauzmann paradox. *The Journal of Chemical Physics*. 1988;88(2):7818-7825.

82. Malandro DL, Lacks DJ. Relationships of shear-induced changes in the potential energy landscape to the mechanical properties of ductile glasses. *The Journal of Chemical Physics*. 1999;110(9):4593-4601.

83. Wales DJ. A Microscopic Basis for the Global Appearance of Energy Landscapes. *Science*. 2001;293(5537):2067-2070.

84. Doye JPK, Wales DJ. Saddle points and dynamics of Lennard-Jones clusters, solids, and supercooled liquids. *The Journal of Chemical Physics*. 2002;116(9):3777-3788.

85. Johnson WL, Samwer K. A Universal Criterion for Plastic Yielding of Metallic Glasses with a $(T/T_g)^{2/3}$ Temperature Dependence. *Physical Review Letters*. 2005;95(19):195501.

86. Chen M. A brief overview of bulk metallic glasses. *NPG Asia Materials*. 2011;3:82-90.

87. Gaskell PH. A new structural model for transition metal–metalloid glasses. *Nature*. 1978;276(5687):484-485.

88. Gaskell PH. A new structural model for amorphous transition metal silicides, borides, phosphides and carbides. *Journal of Non-Crystalline Solids*. 1979;32(1-3):207-224.

89. Gaskell PH. Medium-range structure in glasses and low-Q structure in neutron and X-ray scattering data. *Journal of Non-Crystalline Solids*. 2005;351(12-13):1003-1013.

90. Dubois JM, Gaskell PH, Le Caer G. A Model for the Structure of Metallic Glasses Based on Chemical Twinning. *Proceedings of the Royal Society of London A: Mathematical, Physical and Engineering Sciences*. 1985;402(1823):323-357.

91. Waseda Y, Chen HS. Structural study of metallic glasses containing boron (Fe-B, Co-B, and Ni-B). *Physica Status Solidi (a)*. 1978;49(1):387-392.

92. Boudreaux DS, Frost HJ. Short-range order in theoretical-models of binary metallic-glass alloys. *Physical Review B*. 1981;23(4):1506.

93. Lamparter P. Reverse Monte-Carlo simulation of amorphous $Ni_{80}P_{20}$ and $Ni_{81}B_{19}$. *Physica Scripta*. 1995;T57:72.

94. Inoue A, Negishi T, Kimura HM, Zhang T, Yavari AR. High Packing Density of Zr-and Pd-Based Bulk Amorphous Alloys. *Materials Transactions*, *JIM*. 1998;39(2):318-321.

95. Wang WH, Wang RJ, Zhao DQ, Pan MX, Yao YS. Microstructural transformation in a $Zr_{41}Ti_{14}Cu_{12.5}Ni_{10}Be_{22.5}$ bulk metallic glass under high pressure. *Physical Review B*. 2000;62(17):11292-11295.

96. Wang R. Short-range structure for amorphous intertransition metal alloys. *Nature*. 1979;278(5706):700-704.

97. Saida J, Matsushita M, Inoue A. Direct observation of icosahedral cluster in $Zr_{70}Pd_{30}$ binary glassy alloy. *Applied Physics Letters*. 2001;79(3):412-414.

98. Kelton KF. Crystal Nucleation in Supercooled Liquid Metals. *International Journal of Microgravity Science and Application*. 2013;30(1):11-18.

99. Miracle DB. A structural model for metallic glasses. *Nature Materials*. 2004;3(10):697-702.

100. Miracle DB. Efficient local packing in metallic glasses. *Journal of Non-Crystalline Solids*. 2004;342(1-3):89-96.

101. Miracle DB, Sanders WS, Senkov ON. The influence of efficient atomic packing on the constitution of metallic glasses. *Philosophical Magazine*. 2003;83(20):2409-2428.

102. Miracle DB. The efficient cluster packing model – An atomic structural model for metallic glasses. *Acta Materialia*. 2006; 54(16):4317-4336.

103. Sheng HW, Luo WK, Alamgir FM, Bai JM, Ma E. Atomic packing and short-to -medium-range order in metallic glasses. *Nature*. 2006;439(7075):419-425.

104. Cheng YQ, Ma E, Sheng HW. Atomic level structure in multicomponent bulk metallic glass. *Physical Review Letters*. 2009;102(24):245501.

105. Cheng YQ, Ma E. Atomic-level structure and structure-property relationship in metallic glasses. *Progress in Materials Science*. 2011;56(4):379-473.

106. Egami T, Waseda Y. Atomic size effect on the formability of metallic glasses. *Journal of Non-Crystalline Solids*. 1984;64(1-2):113-134.

107. Senkov ON, Miracle DB. Effect of the atomic size distribution on glass forming ability of amorphous metallic alloys. *Materials Research Bulletin*. 2001;36(12):2183-2198.

108. Frank FC, Kasper JS. Complex alloy structures regarded as sphere packing. I. Definitions and basic principles. *Acta Crystallographica*. 1958;11(3):184-190.

109. Clarke AS, Jónsson H. Structural changes accompanying densification of random hard-sphere packings. *Physical Review E*. 1993;47(6):3975-3984.

110. Almyras GA, Lekka CE, Mattern N, Evangelakis GA. On the microstructure of the $Cu_{65}Zr_{35}$ and $Cu_{35}Zr_{65}$ metallic glasses. *Scripta Materialia*. 2010;62(1):33-36.

111. Almyras GA, Papageorgiou DG, Lekka CE, Mattern N, Eckert J, Evangelakis GA. Atomic cluster arrangements in Reverse Monte Carlo and Molecular Dynamics structural models of binary Cu–Zr metallic glasses. *Intermetallics*. 2011;19(5):657-661.

112. Antonowicz J, Pietnoczka A, Drobiazg T, Almyras GA, Papageorgiou DG, Evangelakis GA. Icosahedral order in Cu-Zr amorphous alloys studied by means of X-ray absorption fine structure and molecular dynamics simulations. *Philosophical Magazine*. 2012;92(15):1865-1875.

113. Lekka CE, Bokas GB, Almyras GA, Papageorgiou DG, Evangelakis GA. Clustering, microalloying and mechanical properties in Cu/Zr-based glassy models by molecular dynamics simulations and ab-initio computations. *Journal of Alloys and Compounds*. 2012;536(Suppl 1):S65-S69

114. Hirata A, Guan P, Fujita T, Hirotsu Y, Inoue A, Yavari AR, et al. Direct observation of local atomic order in a metallic glass. *Nature Materials*. 2011;10(1):28-33.

115. Xi XK, Li LL, Zhang B, Wang WH, Wu Y. Correlation of atomic cluster symmetry and glass-forming ability of metallic glass. *Physical Review Letters*. 2007;99(9):095501.

116. Fujita T, Konno K, Zhang W, Kumar V, Matsuura M, Inoue A, et al. Atomic-scale heterogeneity of a multicomponent bulk metallic glass with excellent glass forming ability. *Physical Review Letters*. 2009;103(7):075502.

117. Cohen MH, Grest GS. Liquid-glass transition, a free-volume approach. *Physical Review B*. 1979;20(3):1077.

118. Grest GS, Cohen MH. Liquid-glass transition: Dependence of the glass transition on heating and cooling rates. *Physical Review B*. 1980;21(9):4113.

119. Egami T. Nano-glass Mechanism of Bulk Metallic Glass Formation. *Materials Transactions*. 2002;43(3):510-517.

120. Dmowski W, Iwashita T, Chuang CP, Almer J, Egami T. Elastic heterogeneity in metallic glasses. *Physical Review Letters*. 2010; 105(20):205502.

121. Wang Z, Wen P, Huo LS, Bai HY, Wang WH. Signature of viscous flow units in apparent elastic regime of metallic glasses. *Applied Physics Letters*. 2012;101(12):121906.

122. Wang DP, Zhu ZG, Xue RJ, Ding DW, Bai HY, Wang WH. Structural perspectives on the elastic and mechanical properties of metallic glasses. *Journal of Applied Physics*. 2013;114(17):173505.

123. Liu ST, Wang Z, Peng HL, Yu HB, Wang WH. The activation energy and volume of flow units of metallic glasses. *Scripta Materialia*. 2012;67(1):9-12.

124. Yu HB, Shen X, Wang Z, Gu L, Wang WH, Bai HY. Tensile plasticity in metallic glasses with pronounced β relaxations. *Physical Review Letters*. 2012;108(1):015504.

125. Liu ST, Jiao W, Sun BA, Wang WH. A quasi-phase perspective on flow units of glass transition and plastic flow in metallic glasses. *Journal of Non-Crystalline Solids*. 2013;376:76-80.

126. Fan C, Liaw PK, Wilson TW, Dmowski W, Choo H, Liu CT, et al. Structural model for bulk amorphous alloys. *Applied Physics Letters*. 2006;89(11):111905.

127. Fan C, Liaw PK, Liu CT. Atomistic model of amorphous materials. *Intermetallics*. 2009;17(1-2):86-87.

128. Fan C, Ren Y, Liu CT, Liaw PK, Yan HG, Egami T. Atomic migration and bonding characteristics during a glass transition investigated using as-cast Zr-Cu-Al. *Physical Review B*. 2011;83(19):195207.

129. Fan C, Liaw PK, Haas V, Wall JJ, Choo H, Inoue A, Liu CT. Structures and mechanical behaviors of $Zr_{55}Cu_{35}Al_{10}$ bulk amorphous alloys at ambient and cryogenic temperatures. *Physical Review B*. 2006;74(1):014205.

130. Fan C, Yan HG, Liu CT, Li HQ, Liaw PK, Ren Y, et al. Changes in the atomic structure through glass transition observed by X-ray scattering. *Intermetallics*. 2012;23:111-115.

131. Zhao J, Inoue A, Liu CT, Liaw PK, Shen X, Pan S, et al. Structure evolution and energy landscape of the clusters in $Zr_{55}Cu_{35}Al_{10}$ metallic liquid and glass. *Scripta Materialia*. 2016;117:64-67.

132. Zhao JF, Tang Z, Kelton KF, Liu CT, Liaw PK, Inoue A, et al. Evolution of the atomic structure of a supercooled $Zr_{55}Cu_{35}Al_{10}$ liquid. *Intermetallics*. 2017;82:53-58.